



# One-dimensional chain copper(II) complex: Synthesis, X-ray crystal structure and catalytic activity in the epoxidation of styrene

Debraj Saha, Tanmoy Maity, Tirthankar Dey, Subratanath Koner\*

Department of Chemistry, Jadavpur University, Kolkata 700032, India

## ARTICLE INFO

### Article history:

Received 1 November 2011

Accepted 27 December 2011

Available online 17 January 2012

### Keywords:

Copper(II)  
Helical chain compound  
Schiff-base complex  
Hydrogen peroxide  
Epoxidation  
Styrene

## ABSTRACT

Two new copper(II) complexes,  $[\text{Cu}(\text{HL}^1)(\text{NO}_3)]$  (**1**) ( $\text{H}_2\text{L}^1 = 1-(N\text{-}ortho\text{-hydroxyacetophenimine})\text{-ethane-2-ol}$ ) and  $\{[\text{Mg}(\text{H}_2\text{O})_6][\text{Cu}(\text{pydca})_2] \cdot 2\text{H}_2\text{O}\}_n$  (**2**) ( $\text{H}_2\text{pydca} = 2,5\text{-pyridine dicarboxylic acid}$ ) have been synthesized and characterized. X-ray crystal structure analysis reveals that the geometry of complex **1** is square planar, where copper(II) centers are linked through a weak coordination by the nitrate O atoms occupying two axial positions, resulting a helical chain structure. Complex **1** crystallizes in the chiral space group  $P2_1$ . There is no chiral center in the Schiff-base ligand of **1**, its helical structure develops due to the formation of a  $\text{NO}_3^-$  bridged chain through an asymmetric arrangement. Complex **2** is a 1D chain in which the copper(II) ions are connected by bridging carboxylato ligands. The  $[\text{Mg}(\text{H}_2\text{O})_6]^{2+}$  moiety occupies the inter-chain space. Epoxidation reactions of styrene and substituted styrenes are homogeneously catalyzed by complexes **1** and **2** with  $\text{H}_2\text{O}_2$  as the oxidant.

© 2012 Elsevier Ltd. All rights reserved.

## 1. Introduction

Epoxidation is one of the most important C=C bond functionalization methods, and the epoxide group is an active intermediate for laboratory syntheses as well as in chemical industries [1–4]. Epoxides can be converted into alcohols, polyethers and aldehydes, which show widespread applications in chemical and pharmaceutical industries [5]. Olefin epoxidation catalyzed by transition metal complexes has been a subject of great interest in the past few decades [6]. Immobilization of transition metal Schiff-base complexes onto zeolitic, polymeric or clay matrices has been adopted to prepare heterogeneous catalysts. Copper(II) Schiff-base complexes, upon immobilization into microporous or mesoporous aluminosilicates, have been found to be capable of catalyzing olefin epoxidations [7–9]. However, attempts of using Schiff-base copper(II) complexes in homogeneous catalytic oxidation are rare in the literature [10–12]. Several oxidants, 30% hydrogen peroxide, *tert*-butyl-hydroperoxide (*tert*-BuOOH), sodium hypochlorite and even molecular oxygen are used for the production of epoxides from alkenes. Amongst them, 30% hydrogen peroxide attracts increased attention in industrial use because it is environmental friendly. In fact, as recently outlined by Beller [13],  $\text{H}_2\text{O}_2$  is characterized by unique features and advantages [14], such as high atom-efficiency [15], moderate cost, safe handling and storage, and production of water as the only by-product [16,17], making

it the most interesting oxidant after molecular oxygen and stimulating its use in liquid-phase oxidations, especially for fine-chemicals production [3].

Styrene oxide is an important organic intermediate for the production of a number of fine/specialty chemicals and pharmaceuticals. The epoxidation of styrene, being a terminal olefin, to styrene oxide is quite difficult and in many cases benzaldehyde or phenylacetaldehyde are produced to a large excess. In the course of our continuing investigation on epoxidation of olefins using heterogeneous and homogeneous catalytic processes, we found transition metal based catalysts demonstrate desirable catalytic efficacy [8,9,11,12]. We report here the synthesis and crystal structure of a 1D helical copper(II) schiff-base complex, namely  $[\text{Cu}(\text{HL}^1)(\text{NO}_3)]$  (**1**) ( $\text{H}_2\text{L}^1 = 1-(N\text{-}ortho\text{-hydroxyacetophenimine})\text{-ethane-2-ol}$ ) and a 1D copper(II) carboxylato complex, namely  $\{[\text{Mg}(\text{H}_2\text{O})_6][\text{Cu}(\text{pydca})_2] \cdot 2\text{H}_2\text{O}\}_n$  (**2**) ( $\text{H}_2\text{pydca} = 2,5\text{-pyridine dicarboxylic acid}$ ), along with their catalytic activity towards the epoxidation of styrene using  $\text{H}_2\text{O}_2$  as the oxidant under homogeneous conditions.

## 2. Experimental

### 2.1. Materials

Ethanolamine, *o*-hydroxyacetophenone and 2,5-pyridine dicarboxylic acid were purchased from Sigma–Aldrich and were used as received. Copper nitrate, magnesium nitrate and solvents used were purchased from Merck (India).

\* Corresponding author. Tel.: +91 33 2457 2778; fax: +91 33 2414 6414.

E-mail address: [snkoner@chemistry.jdvu.ac.in](mailto:snkoner@chemistry.jdvu.ac.in) (S. Koner).

## 2.2. Synthesis of the Schiff base ( $H_2L^1$ )

This Schiff-base was prepared as reported previously, with some modifications [18]. In this process a 10 mL methanolic solution of 2-ethanolamine (0.061 g, 1 mmol) and *o*-hydroxyacetophenone (0.136 g, 1 mmol) were mixed together in a flat-bottomed flask. The resulting solution was then refluxed for 30 min, and then cooled to room temperature. Methanol was then separated almost completely from the mixture by using a rotary evaporator. On storing in a refrigerator overnight, a crystalline yellow solid product was obtained and characterized. *Anal. Calc.* for  $C_{10}H_{13}NO_2$ : C, 66.98; H, 7.31; N, 7.83. *Found:* C, 67.1; H, 7.1, N, 7.7%. IR (KBr disk,  $cm^{-1}$ ):  $\nu$ (azomethine) 1610.

## 2.3. Synthesis of the complex $[Cu(HL^1)(NO_3)]_n$ (**1**)

A 10 mL methanolic solution of  $Cu(NO_3)_2 \cdot 3H_2O$  (0.241 g, 1 mmol) was added dropwise to a 10 mL methanolic solution of  $H_2L^1$  (0.179 g, 1 mmol). The solution was then stirred vigorously for only 5 min at room temperature. The resulting deep green mixture was then filtered. The filtrate thus obtained was kept undisturbed at room temperature. On slow evaporation of the filtrate deep bluish green block crystals appeared after 2 days. The crystals were collected by filtration. The compound is hygroscopic so it was stored in  $CaCl_2$  desiccator. *Anal. Calc.* for  $C_{10}H_{12}N_2O_5Cu$ : C, 39.50; H, 3.98; N, 9.21. *Found:* C, 39.7; H, 3.6; N, 9.3%.

## 2.4. Synthesis of the complex $\{[Mg(H_2O)_6][Cu(pydc)_2] \cdot 2H_2O\}_n$ (**2**)

Complex **2** was prepared through a hydrothermal route. It was grown as a green block crystal (yield 55%) in a 20 mL Teflon-lined Parr acid digestion bomb at 170 °C for 5 days, followed by slow cooling at the rate of 10 °C/h to room temperature. For digestion,  $Cu(NO_3)_2 \cdot 6H_2O$ ,  $Mg(NO_3)_2 \cdot 6H_2O$ , 2,5-pyridine dicarboxylic acid ( $H_2pydca$ ), LiOH and Milli-Q water were added in the molar ratio of 2:1:2:1:500. The crystals thus formed were collected and dried in air. *Anal. Calc.* for  $C_{14}H_{22}CuMgN_2O_{16}$ : C, 29.88; H, 3.94; N, 4.98. *Found:* C, 30.1; H, 3.7; N, 4.8%.

## 2.5. Physical measurements

Elemental analysis was performed using a Perkin-Elmer 240C elemental analyzer. Fourier transformed IR spectra ( $4000\text{--}400\text{ cm}^{-1}$ ) of KBr pellets were recorded at 300 K on a Perkin-Elmer RX1 FT-IR spectrometer. TG-DT (Thermo-Gravimetric and Differential Thermal) analysis was made using a Perkin-Elmer (SINGAPORE) Pyris Diamond TG/DTA unit. The heating rate was programmed at  $5\text{ }^\circ\text{C min}^{-1}$  with a protecting stream of  $N_2$  flowing at a rate of  $150\text{ mL min}^{-1}$ . The products of the catalytic reactions were identified and quantified by a Varian CP-3800 Gas Chromatograph using a CP-Sil 8 CB capillary column.

## 2.6. X-ray crystallography

X-ray diffraction data for **1** and **2** were collected on a Bruker SMART APEX CCD X-ray diffractometer using graphite-monochromated Mo  $K\alpha$  radiation ( $\lambda = 0.71073\text{ \AA}$ ). Determination of integrated intensities and cell refinement were performed with the SAINT [19] software package using a narrow-frame integration algorithm. An empirical absorption correction (SADABS) [20] was applied. The structures were solved by direct methods and refined using the full-matrix least-squares technique against  $F^2$  with anisotropic displacement parameters for non-hydrogen atoms with the programs SHELXS97 and SHELXL97 [21]. Hydrogen atoms were placed at calculated positions using suitable riding models with isotropic displacement parameters derived from their carrier atoms. In the

**Table 1**  
Crystal data and structure refinement parameters for complexes **1** and **2**.

Complex	<b>1</b>	<b>2</b>
Formula	$C_{10}H_{12}N_2O_5Cu$	$C_{14}H_{22}CuMgN_2O_{16}$
Formula weight	303.77	562.20
Crystal system	monoclinic	triclinic
Space group	$P2_1$	$P\bar{1}$
<i>a</i> (Å)	8.3180(10)	7.2742(3)
<i>b</i> (Å)	8.0526(10)	7.5120(4)
<i>c</i> (Å)	9.6984(2)	10.7141(5)
$\alpha$ (°)	90.00	80.059(2)
$\beta$ (°)	114.0590(10)	74.5000(10)
$\gamma$ (°)	90.00	69.4630(10)
<i>V</i> (Å <sup>3</sup> )	593.179(16)	526.29(4)
<i>Z</i>	2	1
<i>D</i> <sub>calc</sub> (g/cm <sup>3</sup> )	1.701	1.774
Absorption coefficient (mm <sup>-1</sup> )	1.856	1.155
<i>F</i> (000)	310	289
Intervals of reflection indices	$-10 \leq h \leq 10$ , $-10 \leq k \leq 9$ , $-12 \leq l \leq 12$	$-9 \leq h \leq 9$ , $-9 \leq k \leq 9$ , $-13 \leq l \leq 13$
Measured reflections	9601	6979
Reflections with $ I  > 2\sigma(I)$	2485	2124
Independent reflections	2591	2330
Final <i>R</i> indices [ $ I  > 2\sigma(I)$ ]	$R_1 = 0.0395$ , $wR_2 = 0.1146$	$R_1 = 0.0287$ , $wR_2 = 0.0786$
<i>R</i> indices (all data)	$R_1 = 0.0408$ , $wR_2 = 0.1157$	$R_1 = 0.0319$ , $wR_2 = 0.0805$
<i>R</i> <sub>int</sub>	0.0210	0.0218
$\Delta\rho_{\text{max}}$ (e Å <sup>-3</sup> )	0.273	0.367
$\Delta\rho_{\text{min}}$ (e Å <sup>-3</sup> )	-0.256	-0.294
Goodness-of-fit (GOF) on <i>F</i> <sup>2</sup>	0.988	1.082

final difference Fourier maps there were no remarkable peaks, except for the ghost peaks surrounding the metal centers. A summary of crystal data and relevant refinement parameters for compound **1** and **2** are given in Table 1.

## 2.7. Catalytic reactions

The catalytic reactions were carried out in a glass batch reactor according to the following procedure. Substrate (10 mmol), solvent (5 mL) and catalysts (2 mg) were first mixed. The mixture was then equilibrated to the desired temperature in an oil bath. After addition of hydrogen peroxide (14.4 mmol, 1.5 equiv.), the reaction mixture was stirred continuously. The reactions were performed in the open air. The products of the epoxidation reactions were collected at different time intervals and were identified and quantified by gas chromatography.

## 3. Result and discussion

### 3.1. IR spectroscopic study

For compound **1** a strong peak appears at  $1605\text{ cm}^{-1}$  (see Supplementary material, Fig. S1) which is attributed to the vibrational band for the azomethine ( $>C=CN-$ ) group. Strong peaks appear in the range  $1300\text{--}1200\text{ cm}^{-1}$  due to the presence of the nitrate ( $-NO_3$ ) group. A broad medium intensity band appears in the range  $3500\text{--}3100\text{ cm}^{-1}$ , ascribed to the  $\nu(OH)$  vibration of the hydroxymethyl group. The peaks appearing around  $2920\text{ cm}^{-1}$  are due to the vibration of methylene ( $-CH_2-$ ) groups. The band at  $528\text{ cm}^{-1}$  is ascribed to the Cu–O vibration of compound **1**.

Compound **2** shows a broad band at  $3472\text{ cm}^{-1}$  (see Supplementary material, Fig. S1), which is attributed to  $\nu(OH)$  of water molecules. The peaks near  $3068\text{ cm}^{-1}$  are due to  $\nu(CH)$  vibrations

of the pyridine ring. The sharp absorption band at  $1626\text{ cm}^{-1}$  is due to a combination of  $\nu(\text{C}=\text{C})$  and  $\nu(\text{C}=\text{CN})$  vibrational bands of the ligand. Several strong  $\nu_{\text{as}}(\text{COO}^-)$  and  $\nu_{\text{s}}(\text{COO}^-)$  bands appear in the region  $1607\text{--}1556\text{ cm}^{-1}$  and at  $1392$  and  $1358\text{ cm}^{-1}$  for **2** indicating the participation of the carboxylic group of  $\text{H}_2\text{pydc}$  in coordination with the  $\text{Cu}(\text{II})$  ion through deprotonation. The band at  $1607\text{ cm}^{-1}$  is assigned to the  $\nu_{\text{as}}(\text{COO}^-)$  vibration and the sharp bands at  $1392$  and  $1358\text{ cm}^{-1}$  are ascribed to the  $\nu_{\text{s}}(\text{COO}^-)$  vibrations. The difference between the asymmetric and symmetric carboxylate stretching [ $\Delta = \nu_{\text{as}}(\text{COO}^-) - \nu_{\text{s}}(\text{COO}^-)$ ] is often used for the correlation of the infrared spectra with the structures of metal carboxylates [22]. These values of  $\Delta$  are approximately  $228\text{ cm}^{-1}$  for monodentate,  $164\text{ cm}^{-1}$  for ionic and  $42\text{ cm}^{-1}$  for bidentate carboxylate groups [23]. The value of  $\Delta$  for **2** is  $249\text{ cm}^{-1}$  ( $1607\text{--}1358\text{ cm}^{-1}$ ) showing monodentate coordination. IR bands at  $1287$ ,  $1268$ ,  $1043$  and  $768\text{ cm}^{-1}$  are due to  $\nu(\text{C}-\text{O})$  and  $\delta(\text{O}-\text{C}-\text{O})$  vibrations of the  $\text{pydca}^{2-}$  ligand. The band at  $513\text{ cm}^{-1}$  may be ascribed to  $\text{Cu}-\text{O}$  vibrations and the band at  $419\text{ cm}^{-1}$  is attributed to  $\text{Cu}-\text{N}$  vibrations of compound **2**. The coordination mode of the ligands  $\text{HL}^{1-}$  and  $\text{pydca}^{2-}$  in complexes **1** and **2**, respectively, are shown in Scheme 1.

### 3.2. Crystal structure of $[\text{Cu}(\text{HL}^1)(\text{NO}_3)]_n$ (**1**)

Compound **1** crystallizes in the chiral space group  $P2_1$  and involves the four-coordinated  $\text{CuNO}_3$  chromophore with a square planar geometry. An ORTEP diagram of **1** with the atom numbering is given in Fig. 1. One nitrogen atom and two oxygen atoms of the Schiff-base and one oxygen atom of the nitrate group form the

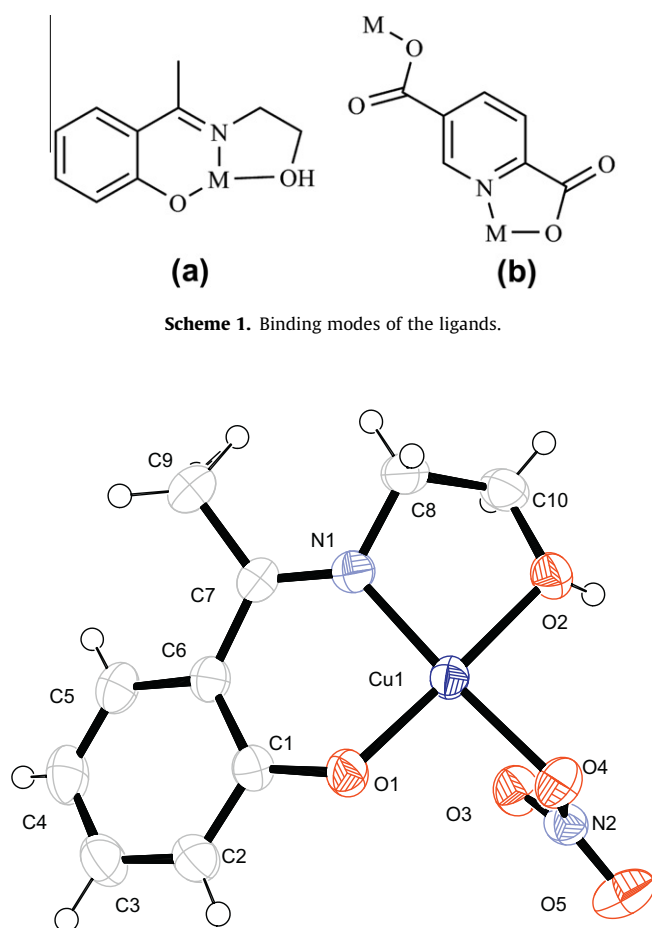


Fig. 1. ORTEP diagram of **1** with 50% ellipsoid probability.

square plane ( $\text{CuONOO}$ ) of the complex (Fig. 1). The four atoms of the square-plane are essentially coplanar, with a slight tetrahedral distortion. The two weakly coordinating oxygen atoms, O3 and O3a ( $a = -1 + x, y, z$ ) from nitrate groups occupy the two axial positions, above and below the  $\text{CuONOO}$  plane with longer bond distances of  $2.587(4)$  and  $2.577(4)\text{ \AA}$ , respectively (Table 2, and Figs. 1 and 2). Such longer bond distances are consistent with weak coordination of the nitrate groups, reported previously [24]. Two weakly coordinated axial oxygen atoms, O3 and O3a ( $a = -1 + x, y, z$ ) from nitrate groups form helical chains parallel to the crystallographic  $b$ -axis (Fig. 2b). The bond distances and bond angles are comparable to other similar types of copper(II) complexes [25,26]. The copper(II) centers of complex **1** are linked through weak coordination by the nitrate O atoms resulting in a helical chain structure, Fig. 2. The crystal packing of complex **1** is further stabilized by intramolecular  $\text{O2}\cdots\text{H6}\cdots\text{O1}$  hydrogen bonding, with an  $\text{O}\cdots\text{O}$  distance of  $2.585(5)\text{ \AA}$ , between the alcoholic oxygen atoms (O2) and hydroxy oxygen atoms (O1) (Fig. 2).

### 3.3. Crystal structure of $\{\text{Mg}(\text{H}_2\text{O})_6\}[\text{Cu}(\text{pydca})_2]\cdot 2\text{H}_2\text{O}\}_n$ (**2**)

X-ray single-crystal analysis reveals that complex **2** has an infinite 1D anionic metal-dicarboxylate ribbon-like chain extending parallel to the crystallographic  $a$ -axis. The 1D coordination

Table 2  
Selected bond lengths ( $\text{\AA}$ ) and angles ( $^\circ$ ) for complexes **1** and **2**.

<b>1</b>		<b>2</b>	
Cu(1)–O(1)	1.890(3)	Cu1–O1	1.9468(14)
Cu(1)–N(1)	1.932(3)	Cu1–N1	1.9757(16)
Cu(1)–O(2)	1.965(4)	Cu1– <sup>c</sup> O3	2.6484(15)
Cu(1)–O(4)	1.990(3)	Cu1– <sup>d</sup> O1	1.9468(14)
Cu(1)–O(3)	2.587(4)	Cu1– <sup>d</sup> N1	1.9757(16)
Cu(1)– <sup>a</sup> O(3)	2.577(4)	Cu1– <sup>e</sup> O3	2.6484(15)
		Mg1–O4	2.0605(16)
		Mg1– <sup>f</sup> O4	2.0605(16)
		Mg1–O5	2.042(2)
		Mg1– <sup>f</sup> O5	2.042(2)
		Mg1–O6	2.0543(18)
		Mg1– <sup>f</sup> O6	2.0543(18)
O(1)–Cu(1)– <sup>a</sup> O(3)	83.49(13)	O1–Cu1– <sup>d</sup> O1	180.00
O(2)–Cu(1)– <sup>a</sup> O(3)	92.05(15)	O1–Cu1–N1	83.24(6)
O(4)–Cu(1)– <sup>a</sup> O(3)	85.02(19)	O1–Cu1– <sup>d</sup> N1	96.76(6)
N(1)–Cu(1)– <sup>a</sup> O(3)	95.0(2)	O1–Cu1– <sup>c</sup> O3	94.54(5)
O(1)–Cu(1)–O(3)	93.53(14)	O1–Cu1– <sup>e</sup> O3	85.47(5)
O(2)–Cu(1)–O(3)	91.03(14)	<sup>d</sup> O1–Cu1–N1	96.76(6)
O(4)–Cu(1)–O(3)	54.98(18)	<sup>d</sup> O1–Cu1– <sup>d</sup> N1	83.24(6)
N(1)–Cu(1)–O(3)	125.04(19)	<sup>d</sup> O1–Cu1– <sup>c</sup> O3	85.47(5)
O(3)–Cu(1)– <sup>a</sup> O(3)	139.91(12)	<sup>d</sup> O1–Cu1– <sup>e</sup> O3	94.54(5)
O(1)–Cu(1)–N(1)	93.20(16)	<sup>c</sup> O3–Cu1– <sup>e</sup> O3	180.00
N(1)–Cu(1)–O(2)	85.39(17)	<sup>c</sup> O3–Cu1–N1	90.33(5)
O(1)–Cu(1)–O(4)	90.52(16)	<sup>c</sup> O3–Cu1– <sup>d</sup> N1	89.67(5)
O(2)–Cu(1)–O(4)	90.87(16)	<sup>e</sup> O3–Cu1–N1	89.67(5)
O(1)–Cu(1)–O(2)	175.20(15)	<sup>e</sup> O3–Cu1– <sup>d</sup> N1	90.33(5)
N(1)–Cu(1)–O(4)	176.26(18)	N1–Cu1– <sup>d</sup> N1	180.00
Cu(1)–O(3)– <sup>b</sup> Cu(1)	115.78(17)	O4–Mg1– <sup>f</sup> O4	180.00
N(2)–O(3)– <sup>b</sup> Cu(1)	109.0(3)	O4–Mg1–O5	92.52(7)
N(2)–O(4)–Cu(1)	106.6(3)	O4–Mg1– <sup>e</sup> O5	87.48(7)
C(7)–N(1)–Cu(1)	127.8(3)	O4–Mg1–O6	89.38(7)
C(8)–N(1)–Cu(1)	108.9(3)	O4–Mg1– <sup>f</sup> O6	90.62(7)
C(1)–O(1)–Cu(1)	123.2(3)	<sup>f</sup> O4–Mg1–O5	87.48(7)
C(10)–O(2)–Cu(1)	111.1(3)	<sup>f</sup> O4–Mg1– <sup>f</sup> O5	92.52(7)
N(2)–O(3)–Cu(1)	79.3(3)	<sup>f</sup> O4–Mg1–O6	90.62(7)
		<sup>f</sup> O4–Mg1– <sup>f</sup> O6	89.38(7)
		O5–Mg1– <sup>f</sup> O5	180.00
		O5–Mg1–O6	90.21(9)
		O5–Mg1– <sup>f</sup> O6	89.79(9)
		<sup>f</sup> O5–Mg1–O6	89.79(9)
		<sup>f</sup> O5–Mg1– <sup>f</sup> O6	90.21(9)
		O6–Mg1– <sup>f</sup> O6	180.00

Symmetry codes: (a)  $1 - x, -1/2 + y, 2 - z$ ; (b)  $1 - x, 1/2 + y, 2 - z$ ; (c)  $-1 + x, y, z$ ; (d)  $-x, 2 - y, 1 - z$ ; (e)  $1 - x, 2 - y, 1 - z$ ; (f)  $-x, 1 - y, -z$ .

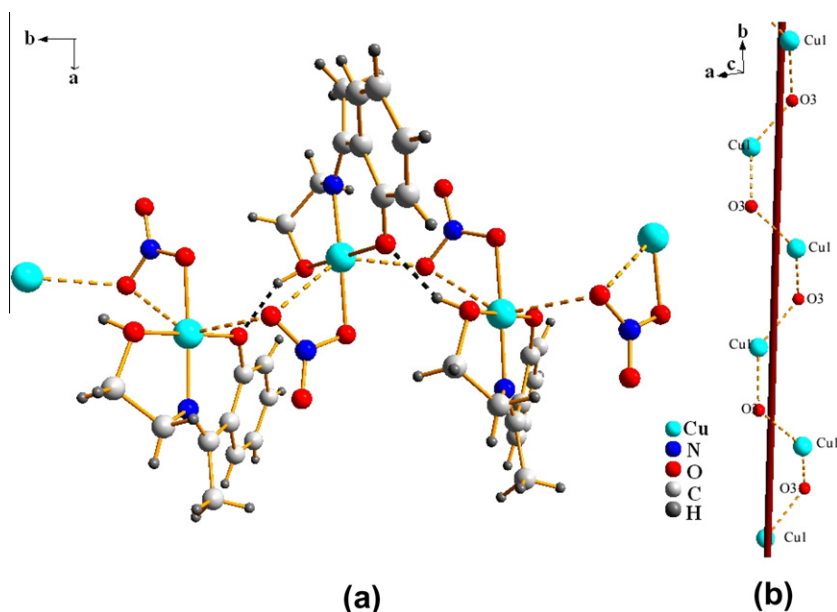


**Fig. 2.** (a) 1D chain of compound **1** with intramolecular H-bonding (yellow dotted lines for secondary interaction and green dotted lines for H-bonding). (b) Helical arrangement of the bridging oxygen atoms of the nitrate around the copper centers in compound **1** (color online).

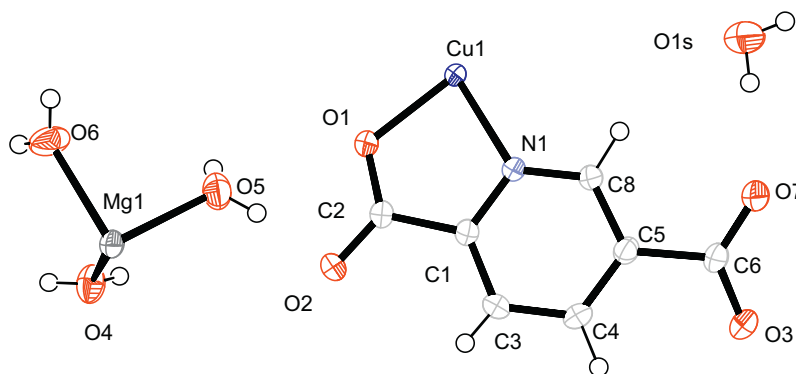


**Fig. 3.** ORTEP diagram of **2** with 50% ellipsoid probability.

polymer contains copper(II) ions connected by pydca dianions, forming  $\{[\text{Cu}(\text{pydca})_2]^{2-}\}_n$  chains. An ORTEP diagram of **2** with the atom numbering is given in Fig. 3. The coordination geometry of copper(II) in **2** is distorted octahedral, which is satisfied by four carboxylato oxygen atoms from four pydca dianions and two pyridine nitrogen atoms of two pydca ligands, Fig. 4. The pyridine nitrogen atom and one of the carboxylato oxygen atoms of the pydca ion ligand form a five-membered ring with the metal. Two nitrogen atoms (N1 and N1d;  $d = -x, 2 - y, 1 - z$ ) and two oxygen atoms (O1 and O1d) from two chelating pydca dianions form the basal plane of the octahedron, while the axial positions are occupied by two oxygen atoms (O3c and O3e;  $c = -1 + x, y, z$ ;  $e = 1 - x, 2 - y, 1 - z$ ) from two different pydca dianions. The bond distances and angles of **2** are collated in Table 2. While the equatorial Cu–O and Cu–N bond distances in compound **2** are comparable, the axial Cu–O bond distances are significantly longer, which is commensurate with the Jahn–Teller sensitive copper(II) ion [27].

The Mg(II) ions are coordinated to six water molecules to form a regular octahedron and afford the cationic part of compound **2** (Fig. 4). The bond distances and angles of **2** are gathered in Table 2. The Mg–O distances vary between 2.042(1) and 2.0605(2) Å, with the O–Mg–O angles being close to 90°. The bond lengths and angles are in agreement with the corresponding values

observed in other  $[\text{Mg}(\text{H}_2\text{O})_6]^{2+}$  containing compounds [28–30]. The  $[\text{Mg}(\text{H}_2\text{O})_6]^{2+}$  ions occupy the space between two adjacent  $\{[\text{Cu}(\text{pydca})_2]^{2-}\}_n$  chains, which are connected to each other through H-bonds mediated by  $[\text{Mg}(\text{H}_2\text{O})_6]^{2+}$  ions forming 2D layers, Fig. 2 (see also Supplementary Material, Fig. S2 and Table S1). Additional reinforcement within the sheet is achieved by other intermolecular O–H...O hydrogen bonds due to the presence of crystalline water molecules in compound **2** (see Supplementary Material, Fig. S2 and Table S1).

#### 3.4. Thermal analysis of compounds **1** and **2**

Thermogravimetric analysis of compound **1** shows a sharp mass loss at around 215 °C (see Supplementary Material, Fig. S3) indicating the decomposition of the complex molecule. As the compound is hygroscopic in nature, we observed weight loss from the starting point of heating. The corresponding DTA curve of compound **1** shows an exothermic peak centered at 215 °C. Thermogravimetric analysis of compound **2** confirms that the compound is thermally stable up to ~70 °C. The TGA curve (see Supplementary Material, Fig. S4) indicates that the mass loss of ~22.4% in the temperature range 70–145 °C corresponds to the loss of two crystalline water molecules and six coordinated water molecules. The corresponding

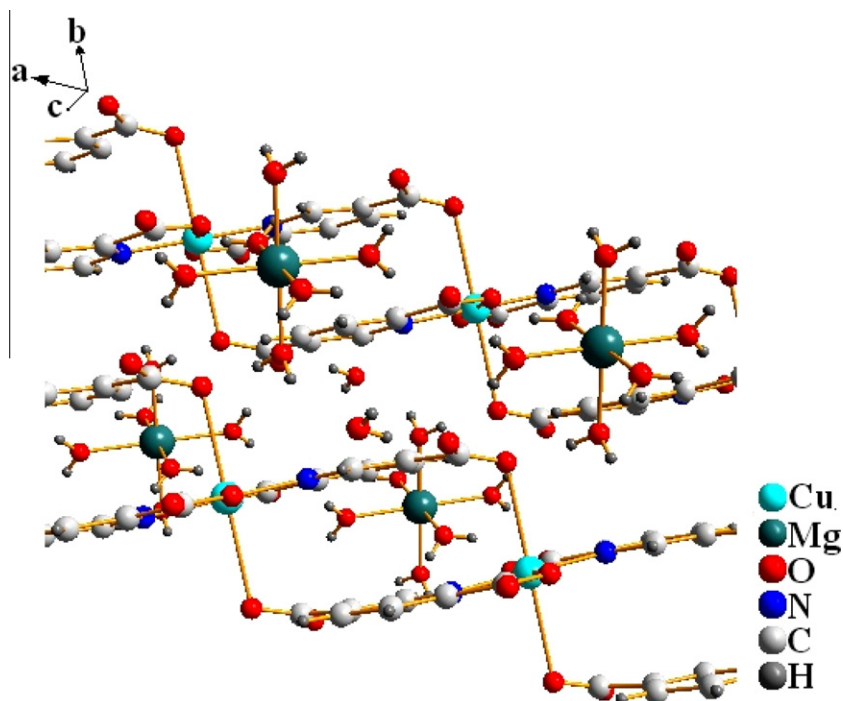


Fig. 4. 1D ribbon of compound 2.

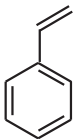
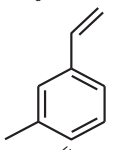
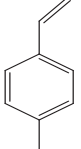
DTA curve of compound **2** shows two endothermic peaks at  $\sim 115$  and  $\sim 140$  °C. Subsequent mass loss indicates the decomposition of the copper-carboxylate moiety.

### 3.5. Catalytic epoxidation reactions

Olefin epoxidation reactions catalyzed by transition metal based catalysts under homogeneous conditions are well documented [6,31]. Seelan et al. studied the epoxidation of styrene over a copper phthalocyanine immobilized NaY catalyst under heterogeneous conditions, which shows over 95% conversion with

epoxide selectivity of  $\sim 24\%$  [32]. Selectivity of the epoxide improves (to  $\sim 53\%$ ) when copper-perchloro-phthalocyanine has been anchored onto MCM-41, however, the conversion remains at 47% [33]. In fact, in the epoxidation of styrene with *tert*-BuOOH over a copper/copper complex immobilized zeolite or with molecular-sieve catalysts, the epoxide selectivity rarely goes above 40% [34]. In our previous attempt we have succeeded in improving the yield of styrene epoxidation up to 86% using a copper(II) Schiff-base anchored MCM-41 catalyst [9]. However, examples of epoxidation reactions homogeneously catalyzed by copper complexes are limited and in many of the cases *tert*-BuOOH was

**Table 3**  
Epoxidation of olefins catalyzed by compounds **1**<sup>a</sup> and **2**.<sup>a</sup>

Substrate	Reaction time (h)	Conversion (wt%)	Epoxide yield (wt%)	TOF <sup>b</sup> (h <sup>-1</sup> )
	(a) 6 (b) 18	(a) 100 (b) 100	(a) 86 (b) 58	(a) 252 (b) 158
	(a) 6 (b) 18	(a) 100 (b) 100	(a) 88 (b) 62	(a) 252 (b) 158
	(a) 6 (b) 18	(a) 100 (b) 100	(a) 92 (b) 65	(a) 252 (b) 158

<sup>a</sup> Reaction conditions: alkenes (10 mmol); catalyst (2 mg); 1.5 mL of 30% H<sub>2</sub>O<sub>2</sub> (14.4 mmol, 1.5 equiv.); solvent (ethanol for compound **1** and acetonitrile for compound **2**) (5 mL). Temperature of the reaction medium was kept at 40 °C for compound **1** and 60 °C for compound **2**. The products of the epoxidation reactions were collected at different time intervals and were identified and quantified by a Varian CP-3800 gas chromatograph equipped with an FID detector and a CP-Sil 8 CB capillary column. Entries (a) and (b) correspond to the catalytic performance of compounds **1** and **2**, respectively.

<sup>b</sup> Turn over frequency (TOF) = moles converted per moles of active site per unit time.

used as the oxidant [10–12]. Rayati et al. studied the epoxidation of styrene over  $[\text{Cu}(\text{hnaphnptn})]$  ( $\text{H}_2\{\text{hnaphnptn}\}$  = Schiff-base derived from the condensation of 2,2'-dimethylpropanediamine and 2-hydroxy-1-naphthaldehyde) and  $[\text{Cu}\{\text{salnptn}(3\text{-OMe})_2\}]$  ( $\text{H}_2\{\text{salnptn}(3\text{-OMe})_2\}$  = Schiff-base derived from the condensation of 2,2'-dimethylpropanediamine and 2-hydroxy-3-methoxybenzaldehyde) under homogeneous conditions using *tert*-BuOOH, which shows over 95% conversion with an epoxide selectivity of ~25% [11]. We have studied this reaction over the Cu(II) Schiff-base complexes  $[\text{Cu}(\text{L}^2)(\text{H}_2\text{O})](\text{ClO}_4)$  ( $\text{HL}^2 = 1\text{-}(N\text{-ortho-hydroxy-acetophenimine})\text{-2-methyl-pyridine}$ ),  $[\text{Cu}(\text{L}^3)]$  ( $\text{HL}^3 = N,N'\text{-}(2\text{-hydroxy-propane-1,3-diyl})\text{-bis-salicylideneimine}$ ) and  $[\text{Cu}(\text{L}^4)]$  ( $\text{HL}^4 = N,N'\text{-}(2,2\text{-dimethyl-propane-1,3-diyl})\text{-bis-salicylideneimine}$ ), which gives styrene epoxide in 54–39% yield (selectivity 72–39%) under homogeneous conditions with *tert*-BuOOH [11]. In this study, styrene and substituted styrene react with  $\text{H}_2\text{O}_2$  to produce epoxides with remarkable selectivity in good yield using compound **1** and **2** under homogeneous conditions. The results of the catalytic epoxidation of different substrates are given in Table 3. The epoxidation of styrene with  $\text{H}_2\text{O}_2$  gives styrene oxide in 100% conversion (selectivity ~86% for **1** and ~58% for **2**); along with this, a small amount of benzaldehyde is also detected. The homogeneous oxidation of 3-Me styrene proceeded smoothly, showing 100% conversion to form 3-Me styrene oxide as the major product with ~88% and ~62% selectivity for **1** and **2** respectively; along with this, 3-Me benzaldehyde was also generated. 4-Me styrene has also been effectively converted to 4-Me epoxystyrene (conversion 100% for both **1** and **2**, selectivity 92% for **1** and 65% for **2**); along with this, 4-Me benzaldehyde was also produced. A high turnover frequency has been attained (~252  $\text{h}^{-1}$  for **1** and ~158  $\text{h}^{-1}$  for **2**) for the epoxide production. A graphical representation of relative efficacy of **1** and **2** for the epoxidation of styrene/substituted styrene with time has been given in Figs. 5 and 6, respectively. The catalytic activity and selectivity in styrene epoxidation over various catalysts containing Cu(II)/Mg(II) under homogeneous conditions are presented in Table 4. It is well known that copper(II) can bind the peroxo-group on treatment with peroxides [35] and the pre-catalyst species containing  $\text{LxCu-OOH}$  (where L = ligand) type moieties seem to be capable of transferring the oxo functionality to the organic substrates to give the corresponding oxidized products [36,37,10]. In our case we propose that a similar kind of mechanism is operative. The X-ray crystal structure analysis of complex **1** shows that the coordination environment around the copper(II)

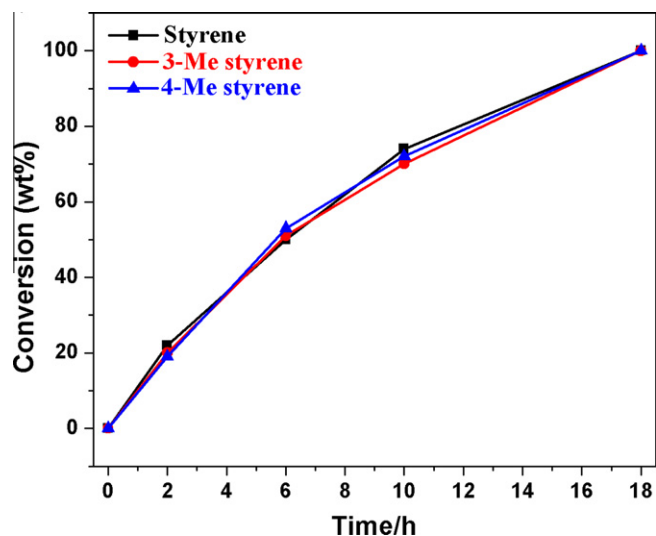


Fig. 6. Kinetic plots for the epoxidation of styrenes catalyzed by compound **2**.

Table 4

Epoxidation of styrene catalyzed by a variety of Cu and Mg-based catalysts under homogeneous conditions using  $\text{H}_2\text{O}_2$ .

Catalyst	Reaction time (h)	Solvent	Temperature ( $^{\circ}\text{C}$ )	Conversion (wt%)	Epoxide yield (wt%)
$\text{Cu}(\text{NO}_3)_2 \cdot 3\text{H}_2\text{O}$	6	$\text{C}_2\text{H}_5\text{OH}$	40	10	12
$\text{Mg}(\text{NO}_3)_2 \cdot 6\text{H}_2\text{O}$	6	$\text{C}_2\text{H}_5\text{OH}$	40	–	–
Compound <b>1</b>	6	$\text{C}_2\text{H}_5\text{OH}$	40	100	86
$[\text{Cu}(\text{OAc})_2 \cdot \text{H}_2\text{O}]$	18	$\text{CH}_3\text{CN}$	60	75	22
Compound <b>2</b>	18	$\text{CH}_3\text{CN}$	60	100	58

ion is easily accessible for an external ligand, as a result hydroperoxide gets enough space to bind copper in the intermediate stages of the catalytic cycle. In complex **2** although the copper(II) ion is hexacoordinated, the peroxo intermediate is formed, maybe due to the replacement at any of its coordination sites. This could be a reason for the higher catalytic activity of compound **1** compared to compound **2**.

The efficacy of different oxidants like *tert*-BuOOH,  $\text{H}_2\text{O}_2$  and NaOCl in compound **1** and compound **2** catalyzed epoxidation reactions of styrene under homogeneous conditions have been studied. The results of this study are given in Table 5 and  $\text{H}_2\text{O}_2$  is found to be the most efficient oxidant. The catalytic reaction was performed in a variety of solvents to study the catalytic efficacy of **1** and **2** in different solvents. The best performance of the catalyst was observed in ethanol for **1** and in acetonitrile for **2** (see Supplementary Material, Table S2). The catalytic efficiency for **1** followed the order: ethanol > methanol > acetonitrile >

Table 5

Epoxidation of styrene with various oxidants over compound **1**<sup>a</sup> and **2**<sup>a</sup>.

Catalyst	Reaction time (h)	Oxidant	Conversion (wt%)	Epoxide yield (wt%)
<b>1</b>	6	None	Not traceable	–
<b>1</b>	6	$\text{H}_2\text{O}_2$	100	86
<b>1</b>	6	<i>tert</i> -BuOOH	62	64
<b>1</b>	6	NaOCl	34	58
<b>2</b>	18	None	Not traceable	–
<b>2</b>	18	$\text{H}_2\text{O}_2$	100	58
<b>2</b>	18	<i>tert</i> -BuOOH	52	52
<b>2</b>	18	NaOCl	28	48

<sup>a</sup> Reaction conditions were the same as given in the footnote of Table 4.

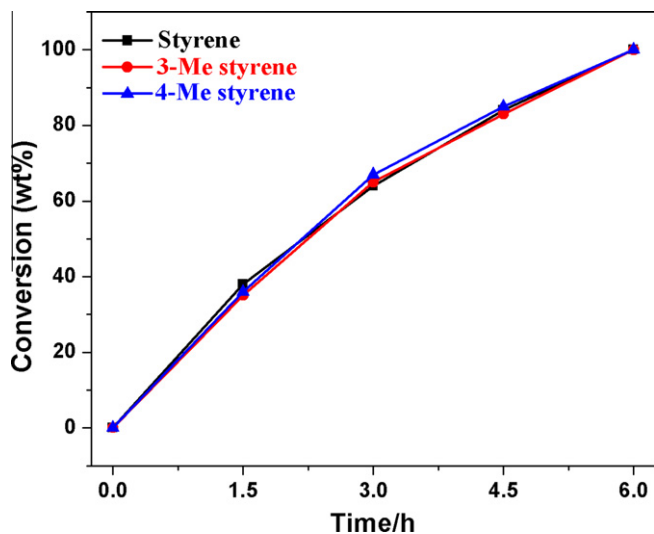


Fig. 5. Kinetic plots for the epoxidation of styrenes catalyzed by compound **1**.

acetone, but for **2** the order was: acetonitrile > acetone > ethanol > methanol. The catalytic reaction was also performed at different temperatures to study the effect on the catalytic efficacy of **1** and **2**. While the best performance was observed for **1** in the temperature range 40–45 °C, for **2** it was 60–65 °C (see Supplementary Material, Table S3).

#### 4. Conclusion

To summarize, we have demonstrated the catalytic efficiency of two newly synthesized and structurally characterized copper complexes in the olefin epoxidation reaction under homogeneous conditions. The catalysts showed good efficiency towards the epoxidation reactions, as reflected by the high turnover frequency of the reactions. The copper Schiff-base compound **1** demonstrates better selectivity towards epoxides than the copper carboxylate compound **2**. This is probably due to the presence of a Lewis acid Mg(II) site in complex **2**-epoxides undergoing an in-situ ring opening reaction to afford side products.

#### Acknowledgements

We acknowledge the Department of Science and Technology (DST), Government of India for funding a project (to S.K.) (SR/S1/IC-01/2009). We also acknowledge DST for funding the Department of Chemistry, Jadavpur University to procure a single crystal XRD machine under the DST-FIST program.

#### Appendix A. Supplementary data

CCDC 817491 and 817490 contain the supplementary crystallographic data for complexes **1** and **2**. These data can be obtained free of charge via <http://www.ccdc.cam.ac.uk/conts/retrieving.html>, or from the Cambridge Crystallographic Data Centre, 12 Union Road, Cambridge CB2 1EZ, UK; fax: (+44) 1223-336-033; or e-mail: [deposit@ccdc.cam.ac.uk](mailto:deposit@ccdc.cam.ac.uk) Supplementary data associated with this article can be found, in the online version, at [doi:10.1016/j.poly.2011.12.039](https://doi.org/10.1016/j.poly.2011.12.039).

#### References

- [1] B.S. Lane, K. Burgess, *Chem. Rev.* 103 (2003) 2457.
- [2] H.C. Kolb, M.S. VanNieuwenhze, K.B. Sharpless, *Chem. Rev.* 94 (1994) 2483.
- [3] R. Noyori, M. Aoki, K. Sato, *Chem. Commun.* (2003) 1977.
- [4] T. Katsuki, *Chem. Soc. Rev.* 33 (2004) 437.
- [5] J.T. Lutz Jr., in: Kirk-Othmer, M. Grayson, D. Eckroth, G.J. Bushey, C.I. Eastman, A. Klingsberg, L. Spiro (Eds.), *Encyclopedia of Chemical Technology*, third ed., vol. 9, Wiley, New York, 1980, pp. 251–266.
- [6] L. Canali, D.C. Sherrington, *Chem. Soc. Rev.* 28 (1999) 85.
- [7] P. Karandikar, M. Agashe, K. Vijayamohan, A.J. Chandwadkar, *Appl. Catal. A* 257 (2004) 133.
- [8] S. Koner, *Chem. Commun.* (1998) 593.
- [9] S. Jana, B. Dutta, R. Bera, S. Koner, *Langmuir* 23 (2007) 2492.
- [10] S. Rayati, S. Zakavi, M. Koliaei, A. Wojtczak, A. Kozakiewicz, *Inorg. Chem. Commun.* 13 (2010) 203.
- [11] C. Adhikary, R. Bera, B. Dutta, S. Jana, G. Bocelli, A. Cantoni, S. Chaudhuri, S. Koner, *Polyhedron* 27 (2008) 1556.
- [12] R. Bera, C. Adhikary, S. Ianelli, S. Chaudhuri, S. Koner, *Polyhedron* 29 (2010) 2166.
- [13] M.K. Tse, S. Bhor, M. Klawonn, G. Anilkumar, H. Jiao, A. Spannenberg, C. Döbler, W. Mägerlein, H. Hugel, M. Beller, *Chem. Eur. J.* 16 (2006) 1875. and references therein..
- [14] J.M. Campos-Martin, G. Blanco-Brieva, J.L.G. Fierro, *Angew. Chem., Int. Ed.* 45 (2006) 6962.
- [15] B.M. Trost, *Angew. Chem., Int. Ed.* 34 (1995) 259.
- [16] G. Strukul (Ed.), *Catalytic Oxidations with Hydrogen Peroxide as Oxidant*, Kluwer Academic, Dordrecht, The Netherlands, 1992.
- [17] G. Grigoropoulou, J.H. Clark, J.A. Elings, *Green Chem.* 5 (2003) 1.
- [18] M. Biswas, G. Pilet, J. Tercers, M.S. El Fallah, S. Mitra, *Inorg. Chim. Acta* 362 (2009) 2915.
- [19] Bruker, APEX 2, SAINT, XPREP, Bruker AXS Inc., Madison, Wisconsin, USA, 2007.
- [20] Bruker, SADABS, Bruker AXS Inc., Madison, Wisconsin, USA, 2001.
- [21] G.M. Sheldrick, SHELXS97 and SHELXL97: Programs for Crystal Structure Solution and Refinement, University of Göttingen, Germany, 1997.
- [22] Z. Vargova, V. Zeleak, I. Cisaova, K. Gyoryova, *Thermochim. Acta* 423 (2004) 149.
- [23] K. Nakamoto, *Infrared and Raman Spectra of Inorganic and Coordination Compounds*, fifth ed., Wiley Interscience, New York, 1997.
- [24] S. Koner, A. Ghosh, N. Ray Chaudhuri, A.K. Mukherjee, M. Mukherjee, R. Ikeda, *Polyhedron* 12 (1993) 1311.
- [25] D.-D. Qin, Z.-Y. Yang, F.-H. Zhang, B. Du, P. Wang, T.-R. Li, *Inorg. Chem. Commun.* 13 (2010) 727.
- [26] C. Adhikary, S. Koner, *Coord. Chem. Rev.* 254 (2010) 2933.
- [27] H. Kumagai, H. Sobukawa, M. Kurmoo, *J. Mater. Sci.* 4 (2008) 2123.
- [28] C.L. Perrin, J.S. Lau, Y.-J. Kim, P. Karri, C. Moore, A.L. Rheingold, *J. Am. Chem. Soc.* 131 (2009) 13548.
- [29] F.E.G. Guner, M. Lutz, T. Sakurai, A.L. Spek, T. Hondon, *Cryst. Growth. Des.* 10 (2010) 4327.
- [30] I.R. Fernando, N. Daskalakis, K.D. Demando, G. Mezei, *New J. Chem.* 34 (2010) 221.
- [31] J.S. Costa, C.M. Markus, I. Mutikainen, P. Gamez, J. Reedijk, *Inorg. Chim. Acta* 363 (2010) 2046.
- [32] S. Seelan, A.K. Sinha, D. Srinivas, S. Sivasanker, *J. Mol. Catal. A* 157 (2000) 163.
- [33] P. Karandikar, M. Agashe, K. Vijayamohan, A. Chandwadkar, *J. Appl. Catal. A* 257 (2004) 133.
- [34] D.E. De Vos, M. Dams, B.F. Sels, P.A. Jacobs, *Chem. Rev.* 102 (2002) 3615.
- [35] T. Osako, S. Nagatomo, Y. Tachi, T. Kitagawa, S. Itoh, *Angew. Chem., Int. Ed. Engl.* 41 (2002) 4325.
- [36] S.T. Prigge, B.A. Eipper, R.E. Mains, L.M. Amzel, *Science* 304 (2004) 864.
- [37] R.A. Ghiladi, K.R. Hatwell, K.D. Karlin, H.-W. Huang, P. Moënné-Loccoz, C. Krebs, B.H. Huynh, L.A. Marzilli, R.J. Cotter, S. Kaderli, A.D. Zuberbühler, *J. Am. Chem. Soc.* 123 (2001) 6183.